



**HAL**  
open science

## **GRAPhEME: a setup to measure $(n, xn\gamma)$ reaction cross sections**

Greg Henning, A. Bacquias, P. Dessagne, M. Kerveno, G. Rudolf, C. Borcea, A. Negret, A. Olacel, J. C. Drohé, A. J. M. Plompen, et al.

### ► To cite this version:

Greg Henning, A. Bacquias, P. Dessagne, M. Kerveno, G. Rudolf, et al.. GRAPhEME: a setup to measure  $(n, xn\gamma)$  reaction cross sections. 4th International Conference on Advancements in Nuclear Instrumentation Measurement Methods and their Applications (ANIMMA), Apr 2015, Lisbon, Portugal. pp.1-9, 10.1109/ANIMMA.2015.7465505 . hal-04417210

**HAL Id: hal-04417210**

**<https://hal.science/hal-04417210>**

Submitted on 26 Jan 2024

**HAL** is a multi-disciplinary open access archive for the deposit and dissemination of scientific research documents, whether they are published or not. The documents may come from teaching and research institutions in France or abroad, or from public or private research centers.

L'archive ouverte pluridisciplinaire **HAL**, est destinée au dépôt et à la diffusion de documents scientifiques de niveau recherche, publiés ou non, émanant des établissements d'enseignement et de recherche français ou étrangers, des laboratoires publics ou privés.

# GRAPhEME: a setup to measure $(n, xn\gamma)$ reaction cross sections

Greg Henning, A. Bacquias, P. Dessagne, M. Kerveno, G. Rudolf  
*IPHC, Université de Strasbourg, 23 rue du Loess 67037 Strasbourg, France,*  
*and CNRS, UMR7178, 67037 Strasbourg, France,*  
 C. Borcea, A. Negret, A. Olacel  
*Nat. Inst. Of Phys. And Nucl. Eng., Bucharest, Romania,*  
 J.C. Drohé, A.J.M. Plompen, M. Nyman  
*EU/ JRC-IRMM, Geel, Belgium.*

**Abstract**—Most of nuclear reactor developments are using evaluated data base for numerical simulations. However, the considered databases present still large uncertainties and disagreements. To improve their level of precision, new measurements are needed, in particular for  $(n, xn)$  reactions, which are of great importance as they modify the neutron spectrum, the neutron population, and produce radioactive species.

In 2003, the IPHC group started an experimental program to measure  $(n, xn\gamma)$  reaction cross sections using prompt gamma spectroscopy and neutron energy determination by time of flight. Measurements of  $(n, xn\gamma)$  cross section have been performed for  $^{235,238}\text{U}$ ,  $^{232}\text{Th}$ ,  $^{\text{nat},182,183,184,186}\text{W}$ ,  $^{\text{nat}}\text{Zr}$ .

The experimental setup, consisting of HPGe detectors and a fission chamber, is installed at the neutron beam at GELINA (Institute for Reference Materials and Measurements (IRMM), Geel, Belgium). It has recently been upgraded with the addition of a highly segmented 36 pixels planar HPGe detector. The setup is equipped with a high rate digital acquisition system. The analysis of the segmented detector data requires a specific procedure to account for cross signals between pixels. An overall attention is paid to the precision of the measurement.

The setup characteristic and the analysis procedure will be presented along with the acquisition and analysis challenges. Examples of results and their impact on models will be discussed. Finally, the perspectives on complimentary experiments will be presented.

## I. CONTEXT AND MOTIVATION

As future nuclear reactor designs and fuel cycles are understudy, the development and risk analysis is mainly done through numerical simulations. These calculations use evaluated nuclear data bases in which are stored the characteristic values (cross section, angular distribution, ...) of all nuclear physics

processes to consider. Such data are evaluated both from experimental measurement and theoretical prediction. However, even today, evaluated data bases still present large uncertainties for many reactions. For example, the cross section for the inelastic neutron scattering off  $^{238}\text{U}$  can differ by as much as 10 % between evaluations – see Fig. 1. These uncertainty lead to uncertainty on the control parameters of reactors ( $k_{\text{eff}}$ , power peak, void, ...) [1]. Theoretical developments and new measurements are necessary to improve the evaluations.

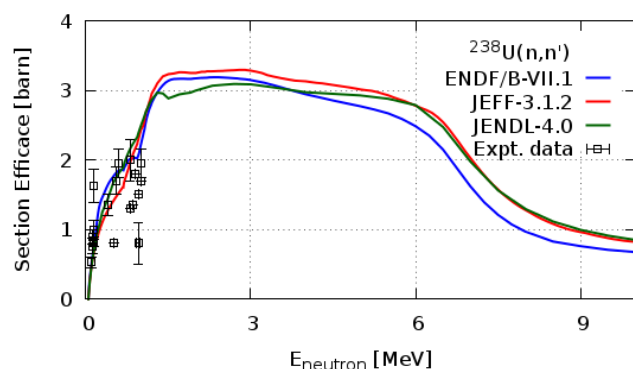


Figure 1. Cross section for the inelastic neutron scattering off  $^{238}\text{U}$  according to the three main evaluations, along with experimental data points. The evaluation differ by as much as 10 % at the top of the cross section. Data and evaluation collected via [2].

Among the reaction of interest for reactor physics, inelastic neutron scattering  $(n, xn)$  is of particular importance as it changes the energy and number of the neutrons. It also creates new isotopes in the material. The direct study of  $(n, xn)$  reaction can be challenging due to the difficulty of detecting

scattered neutron and measuring their energy. But the exclusive  $(n, xn\gamma)$  reaction can be a useful proxy. In  $(n, xn\gamma)$  reaction, it is possible to unequivocally identify the nucleus excited in the reaction by selecting the gamma ray energy corresponding to a transition between states in the nucleus. Ideally, one can collect the total flux of transition going to the ground state of the nucleus and thus infer the total  $(n, xn)$  cross section. However, this is rarely possible. Therefore, one has to rely on models to complete the missing information. As  $(n, xn\gamma)$  cross sections are very strong constrains on models, the experimental measurements are used to tune models and ensure a correct description of the reaction mechanisms. One builds confidence in the models that way.

## II. THE GRAPHEME SETUP

The GRAPhEME (GeRmanium array for Ac-tinides PrEcise MEasurement) setup is installed at the neutron beam facility GELINA, at the European Commission Joint Research Center's Institute for Reference Materials and Measurements in Geel, Belgium [3], [4].

The neutron source is based on a linear electron accelerator producing electron beams. The accelerated particles produce Bremsstrahlung in an uranium target which in turn, by photonuclear reactions, produce neutrons, with an average flux of  $3.4 \times 10^{13}$  neutrons/s. The neutron energy distribution ranges from subthermal to about 20 MeV, with a peak around 1-2 MeV. The flight paths, symmetrically arranged around the uranium target, lead to several experimental locations at distances of 10 to 400 m.

The GRAPhEME setup (Fig. 2) is located 30 meters away from the neutron production target and consists of a fission chamber (FC) to measure the incoming neutron flux and HPGe detectors for the detection of  $\gamma$  rays. The FC is a  $\approx 320 \text{ cm}^3$  volume, filled with a 10 % methane- and 90 % argon-mixture at 1 atm pressure, with a  $^{235}\text{U}$  enriched (99.5 %)  $\text{UF}_4$  deposit 640 nm thick. The reaction of neutrons with the  $^{235}\text{U}$  nuclei induces fission and one of the fission fragment is detected in the gas chamber. The efficiency of the FC has been determined to be  $94.4 \pm 2.1 \%$  [5], [6]. An energy cut allows the differentiation between alpha emission and fission fragment.

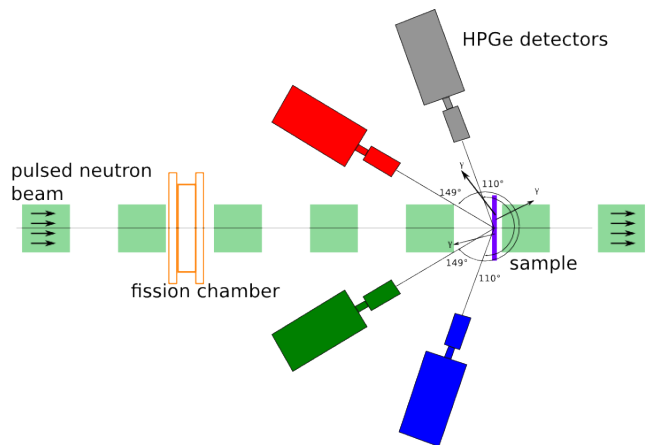


Figure 2. Schematic representation of the GRAPhEME setup with four germanium detectors in the beam plane.

After the fission chamber, planar HPGe detectors surround the sample to study. The average resolution of the detector at 122 keV is 0.75 keV and the absolute efficiency is 0.01.

A close attention has been made to shield the detectors from outside background. In particular from  $\gamma$  rays and neutrons from neighboring beam lines. That is why the sample and the HPGe detectors are enclosed into shield wall of 3 cm-thick lead bricks. To absorb X-rays from the lead, the inside of the shielding is lined with a combination of Cadmium and Copper.

The electron beam used to produce the neutrons is accelerated by a pulsed linear accelerator powered by three high-power klystrons. Being only 30 meters from the production target, our setup is sensitive to the radiated electromagnetism perturbation from the klystrons. For low energy gamma rays, the EM perturbation affects the timing of the signal. To avoid distorting the time spectrum of detected gamma rays, great effort have been spent to ensure the maximum shielding against EM effects. The double shielded signal cables are carefully wrapped in wire mesh and fixed to the support table to avoid any current loops.

The detectors are connected to TNT acquisition cards [7], [8], developed at IPHC. They have 4 inputs for signal, and NIM inputs that allow a synchronization with the neutron beam production. The energy is computed from the detector signal using a Jordanov trapezoidal shaping [9]. The cards' clock are synchronized together. They are connected to a computer via USB cable. The acquisition records in list mode the energy of the detected gamma ray (or

fission fragment) and the time of the event. The time difference between the accelerator pulse ( $T_0$ ) and the detection gives, knowing the distance of flight, the energy of the neutron that induced the reaction.

### III. PRINCIPLE OF $(N, xN\gamma)$ MEASUREMENTS

#### A. Incident neutron energy from Time-of-Flight measurement

The energy of the incident neutron is determined by time of flight. The moment of production of the neutrons is well known from the accelerator pulse of electron on the production target. The distance from the production target to the studied sample has been determined with a precision of 0.001 m (0.03 ‰). The energy of the neutron is calculated with the formula :

$$E_n = m_n c^2 \sqrt{\frac{1}{1 - \left(\frac{DoF/ToF}{c}\right)^2}}$$

where  $m_n$  is the mass of the neutron,  $c$  the speed of light in vacuum,  $DoF$  the distance of flight of the neutron between the production target and the sample in GRAPHEME and  $ToF$  is the time of flight of the neutron.

#### B. Neutron flux determination

The incident neutron flux is determined with the fission chamber located upstream from the sample to study. The geometry, pressure and voltage bias of the ionization chamber were optimized with simulations and the efficiency was precisely calibrated at the Physikalisch-Technische Bundesanstalt (PTB) [5], [6]. The incident neutron flux is extracted from the number of detected fission events via the ratio to the  $^{235}\text{U}(n, f)$  cross section. The neutron flux at GELINA is shown in Fig. 3.

#### C. Gamma ray intensity

Data analysis produces typical 2D time-of-flight vs.  $E_\gamma$  plot like in Fig. 4, in which one notices a constant radioactivity background, and an intense peak of events at very low time of flight. It corresponds to the *gamma flash*, i.e. the detection of gamma rays emitted at the neutron production target, and traveling, at the speed of light along the beam path. Only about 500 nanoseconds after the gamma flash do the most energetic (fastest) neutrons arrive on

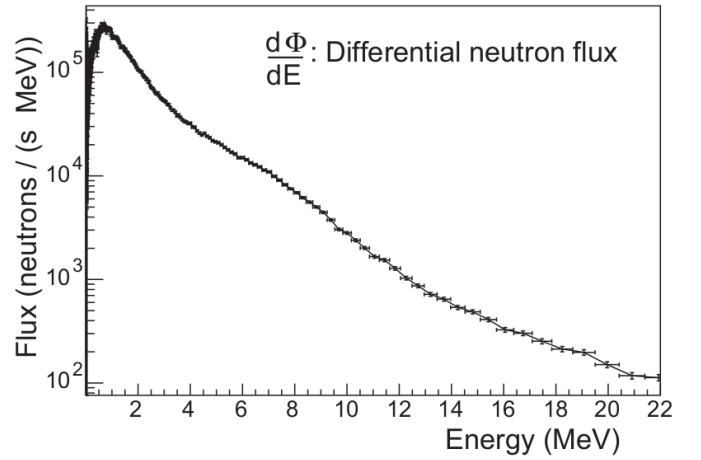


Figure 3. Differential neutron flux measured with the GRAPHEME setup at the 30 meters station on the GELINA flight path (FP16).

the sample and induce reactions. The  $\gamma$ -ray energies corresponding to specific transitions in the nuclei produced in the reaction are clearly visible and can be attributed to the reaction channels:  $(n, n')$ ,  $(n, 2n)$ , and  $(n, 3n)$

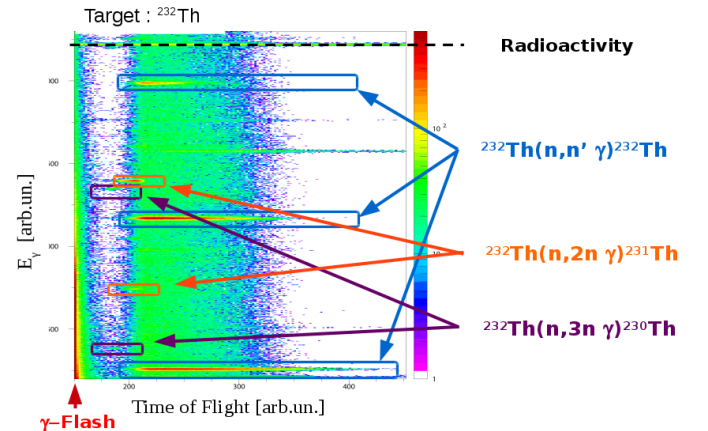


Figure 4. Typical 2D plot of the recorded data with GRAPHEME (here, example on a  $^{232}\text{Th}$  target):  $E_\gamma$  vs. Time-of-Flight. The contribution of the gamma flash and the constant radioactivity background can easily be removed from the gamma line corresponding to neutron induced reaction.

#### D. Differential cross section extraction

The differential cross section  $\frac{d\sigma}{d\Omega}(E_n, \gamma; \theta)$  for a given gamma transition is computed from the intensity of the gamma ray transition at a given time of flight (i.e. at a given neutron energy) and the neutron flux at this particular energy :

$$\frac{d\sigma}{d\Omega}(E_n, \gamma; \theta) = \frac{N_\gamma(E_n; \theta)}{\varepsilon(E_\gamma)} \frac{\sigma_{^{235}\text{U}(n, f)}(E_n) \varepsilon_{\text{FC}}}{N_{\text{target}} N_{\text{FC}}}$$

where  $N_\gamma(E_n; \theta)$  is the number of detected  $\gamma$  rays for the transition,  $\varepsilon(E_\gamma)$  the efficiency of detection for this  $\gamma$  ray,  $\sigma_{235\text{U}(n, f)}(E_n)$  the fission induced cross section of  $^{235}\text{U}$ ,  $\varepsilon_{\text{FC}}$  the detection efficiency of the fission chamber,  $N_{\text{target}}$  the number of isotope of interest in the sample and  $N_{\text{FC}}$  the number of events detected by the fission chamber.

### E. Angle integration

Emitted gamma rays in the neutron induced reaction have specific angular distribution according to their multipolarity. Due to the anisotropic emission it is necessary to correct the detection efficiency to get the actual transition cross section. To do that, we use the Gaussian quadrature method as described in [10], [11]. For transition of multipolarity smaller than 3, two detectors are enough to account for the angular emission anisotropy. The total cross section is

$$\sigma_{\text{total}} = 4\pi \left[ w_1 \frac{d\sigma}{d\Omega}(\theta_1) + w_2 \frac{d\sigma}{d\Omega}(\theta_2) \right]$$

where  $\theta_1 = 149.4^\circ$ ,  $\theta_2 = 109.9^\circ$  and  $w_1 = 0.3749$ ,  $w_2 = 0.6521$ . Even for extended sources and detectors, this relation stays true.

### F. Uncertainties

A great attention is given to sources of uncertainty in order to reduce them as much as possible and have a good knowledge of the precision of the measurement.

The efficiency of the Germanium detectors must be precisely determined. This is done with the use of calibrated sources of  $^{152}\text{Eu}$  placed at the sample position. This data from punctual and extended sources is used to carefully simulate the detectors in MCNP [12] and Geant4 [13]. These simulations are then used to compute the detection efficiency for an extended source of the size of the beam spot on the sample. The absorption of  $\gamma$  rays in the target material is also taken into account.

The fission chamber efficiency is determined with precision (see above). The neutron energy precision depends on the 10 ns sampling period of the acquisition electronic. Thus, a precision down to 10 keV can be achieved for a 1 MeV neutron, but the limit of resolution for a 10 MeV neutron is 300 keV. Also, the lower flux at high neutron energy increases the statistical error above 10 MeV.

Finally, it is very important to know well the characteristic of the sample. The absolute mass of isotope of interest is obviously necessary to normalized correctly the measured cross section. But, for the calculation of auto absorption, a good knowledge of the target thickness, contaminants and density is also needed. Indeed, surface or deep oxidation will change the density of matter and lead to more or less absorption of gamma rays emitted from within the target. The use of precise measurement, weighting, polishing at the IRMM, and electron imagery at the Institute for Transuranium Elements (ITU) is helpful to that end.

To conclude, a precision of 5 % to 15 % on the reaction cross section can be achieved, depending on the gamma energy, neutron energy and cross section.

### G. Studied systems and impact on theories

Many system have been studied with GRAPHEME. Table I summarizes the isotopes, year of measurement and the total acquisition time for which experimental data is recorded.

Isotope	Year	Total acq. time
$^{235}\text{U}$	2010	61 days
$^{238}\text{U}$	2012	120 days
$^{232}\text{Th}$	2009 & 2013	16 days
$^{\text{nat}}\text{W}$	2009 & 2014	24 days
$^{182}\text{W}$	2011	42 days
$^{183}\text{W}$	2012	60 days
$^{184}\text{W}$	2011	25 days
$^{186}\text{W}$	2010	15 days
$^{\text{nat}}\text{Zr}$	2014	80 days
$^{233}\text{U}$	2014 - 2015	30 days

Table I  
SUMMARY OF ISOTOPES STUDIED WITH GRAPHEME.

With the  $^{235}\text{U}$  sample, for example, only 4 transitions (one for the (n, n') channel, three for the (n, 2n) channel) could be studied because of the high radioactivity and neutron induced fission background. A better agreement between experimental data and calculation has been found for phenomenological entrance channels models [14], [15], [16], [5].

For the isotope  $^{238}\text{U}$ , 35 (n, n' $\gamma$ ) transitions were studied, with varying degrees of agreement with calculations [15], [16]. The study of  $^{238}\text{U}$  is challenged by the difficulty to extract a cross section for the transition from the first excited state to the ground state, with an energy of 45 keV, that is

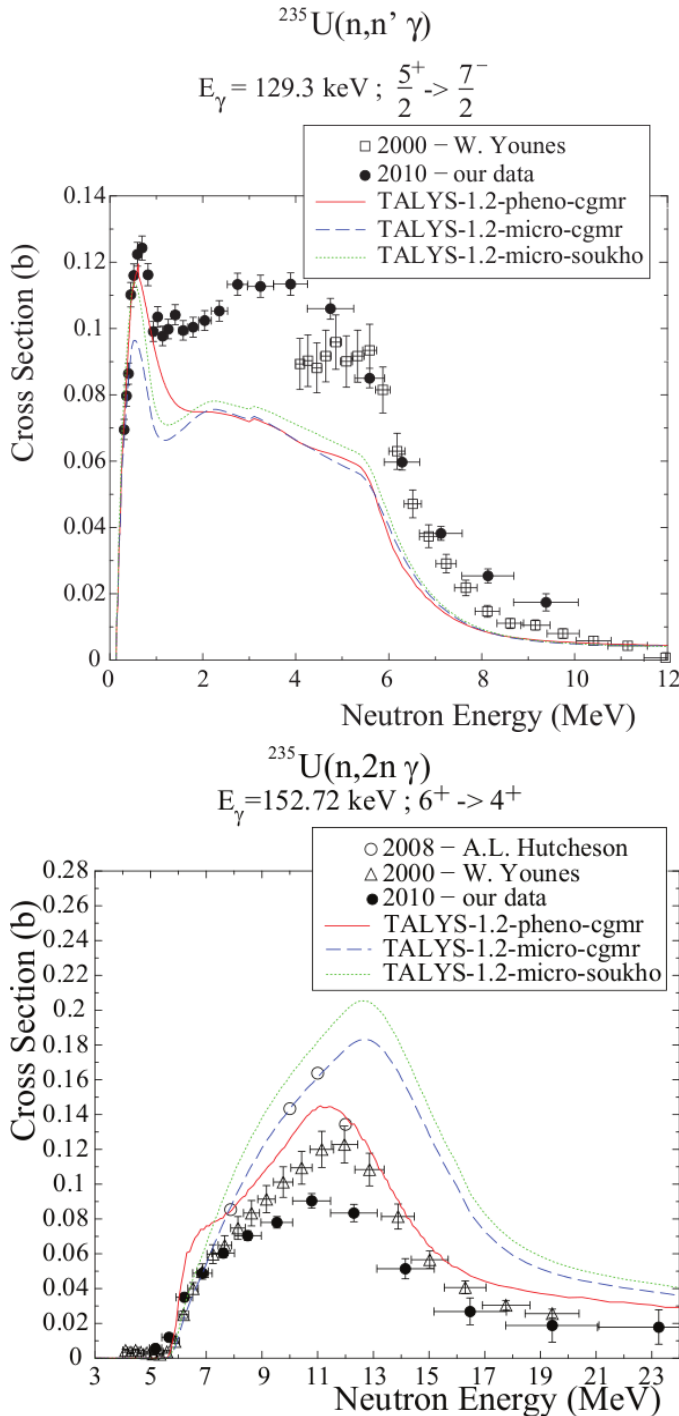


Figure 5. Examples of results obtained with GRAPhEME for  $^{235}\text{U}$ . (Top) Experimental cross section for a  $\gamma$  transition in  $^{235}\text{U}$  in  $(n, n')$  reaction, compared to theoretical predictions from TALYS calculations. (Bottom) Same for a  $(n, 2n)$  reaction. From [14].

strongly converted. The uncertainty on the sample characteristics was also a limitation. The sample  $^{238}\text{U}$  absolute mass was given with a 20 % uncertainty only by the provider. This is too much for our precision goal. In fact, the effective density of the sample was found to be  $15 \text{ g/cm}^3$ , significantly below the expected  $19 \text{ g/cm}^3$  of metallic uranium. Important efforts were spent to get a more precise measurement of the total mass of the isotope of interest. First, the sample was weighted with a 0.1 mg precision (0.02 %) at the IRMM target preparation laboratory, after brushing the surface to remove any oxides. Electron microscopy imagery was performed at ITU and revealed a very uneven surface, explaining the low density. Finally, a measurement of the  $^{238}\text{U}$  content was performed via  $\gamma$  spectroscopy on the 1001.03 keV line in the radioactivity decay chain of the nucleus. This last method allowed a determination of the isotope total mass with a precision better than 2 % [17].

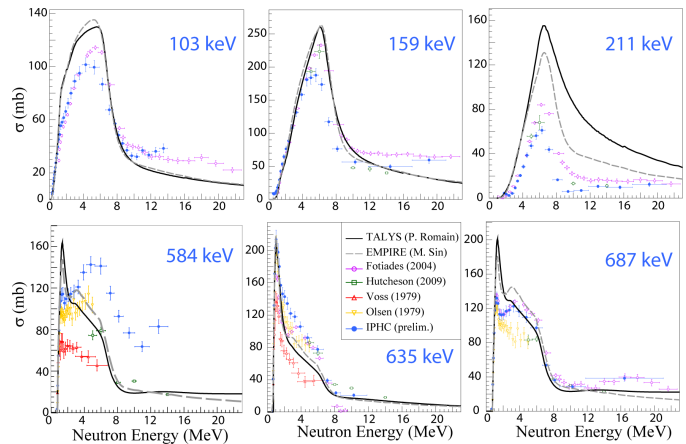


Figure 6. Example of some of the  $^{238}\text{U}(n, n' \gamma)$  transition cross sections studied with GRAPhEME, compared to other experimental results and theoretical models [15]. In total, 35  $(n, n' \gamma)$  cross sections were obtained (see text).

The measured cross sections are compared to theoretical predictions, calculated with reaction codes, like TALYS [18] or EMPIRE [19]. It is a good way to point the weakness of the models. For example, the impact of structure parameters on the predicted cross sections has been identified. Indeed, the reaction codes use level scheme information to be able to calculate  $(n, xn\gamma)$  cross sections; however, the structure database present large uncertainty on branching ratio for some transitions in many nuclei, including  $^{238}\text{U}$ . The effect of these uncertainties has been estimated to have an impact of up to 10 %

on cross sections. Moreover, the reaction codes arbitrarily limit the number of discrete levels taken into account in the calculation. This has an impact on the shape of the cross section – see figure 7.

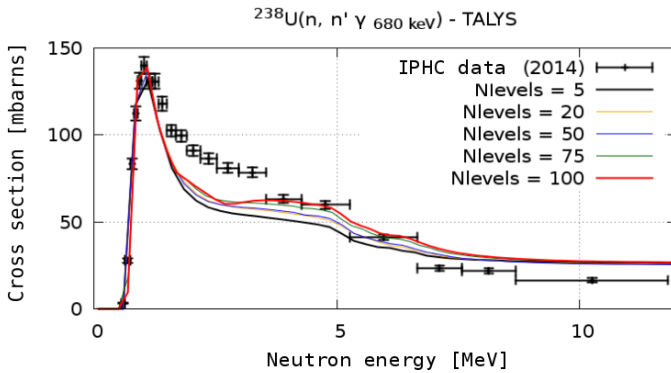


Figure 7. Example of a cross section for  $^{238}\text{U}(n, n'\gamma)$  studied with GRAPhEME using more and more discrete levels in TALYS-1.6 calculations [20].

The importance of the reaction mechanisms has also been identified. Quasiparticle Random Phase Approximation (QRPA) calculations in the entrance channel by M. Dupuis (CEA/DAM) [21] tend to produce spin distribution centered on lower values than with the usual exciton model. The use of this microscopic calculation can fix some important disagreement between calculations and measurement in some transitions – for example, see Fig. 8.

#### IV. SEGMENTED GERMANIUM

To cope with the high background from very radioactive samples (like  $^{233}\text{U}$ ,  $^{239}\text{Pu}$ ), a segmented germanium detector was added to the setup, in order to increase the granularity, and thus reduce the sensitivity to the gamma flash and radioactivity.

The detector Ge crystal is 54 mm by 54 mm, 20 mm thick, segmented into 6 by 6 grid, with squared pixels 6.66 mm wide. Each pixel has its own pre-amplification stage. The crystal is enclosed in an aluminum casing, step shaped to allow it to get closer to the beam – see photography of Fig. 9. The detector was built by CANBERRA. It has been characterized precisely using calibrated source, and simulated within a GEANT4 simulated geometry – see Fig. 9, bottom. The simulations and test measurements agree within 5 % as of today – see Fig. 10. At low  $\gamma$  energy ( $\lesssim 100$  keV), some discrepancies remain (Fig. 10, top) due to the incomplete inclusion of all materials present in the detector nose which is not known precisely

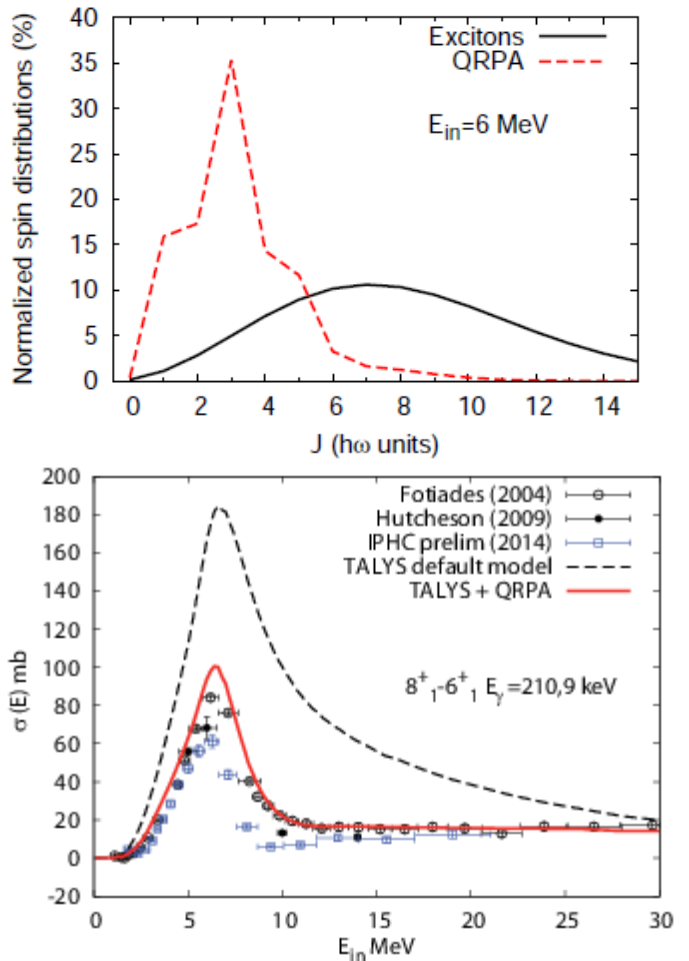


Figure 8. QRPA calculations by M. Dupuis. (Top) Spin distribution of states populated in the entrance channel calculated by the QRPA approach, compared to the exciton model. (Bottom) Results of  $(n, n'\gamma)$  calculations for the 210 keV transition in the g.s. band of  $^{238}\text{U}$ , calculated using the exciton model (black, dashed) or with the QRPA approach (red continuous), compared to experimental values [21].

either in dimension, location or composition (Teflon, electronic component, ...). Special consideration is to be given to electric cross talk between pixels (mirror charges), as well as scattering of gamma rays from one pixel to the other. Simulations suggest that 20 % of single gamma hitting the detector are leading to a multiplicity of hit pixels of 2 or more. Most (50 %) of the scattered gamma are detected in the closest neighboring pixels, but the scattering is observed with distances up to the size of the Ge crystal– see Fig. 11. A specific processing is being developed to take those particular case, specific to segmentation, into account in the data analysis. It is important, for example to ensure that measured energy in a pixel is not perturbed by mirror charges from neighboring pixels.

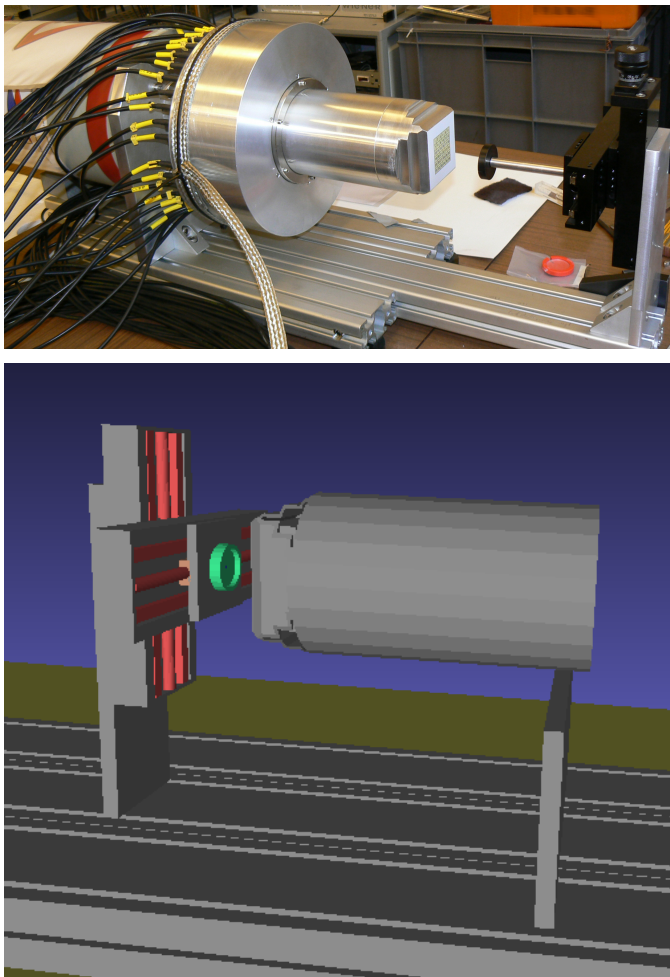


Figure 9. (Top) Photography of the segmented Ge detector on its test bench. (Bottom) Simulated geometry on Geant4 of the Segmented germanium detector.

The Segmented germanium detector was added into the GRAPhEME setup in autumn 2014 and used to start taking data on  $^{233}\text{U}$ . It already demonstrated its helpfulness in coping with the high radioactivity background from this isotope.

## V. PERSPECTIVES

### A. Conversion electron spectroscopy

For highly converted transition in actinides (such as the decay of the  $2_1^+$  state to the g.s. in  $^{238}\text{U}$ , with an energy  $E_\gamma = 45$  keV), the prompt gamma-ray method is difficult to apply, as only a few gamma rays can be detected, even for intense transitions in the level scheme. Therefore, we are studying the possibility to perform conversion electron spectroscopy. This method implies new challenges, such as using a very thin target (to allow the escape of electrons) and working under vacuum, with a well

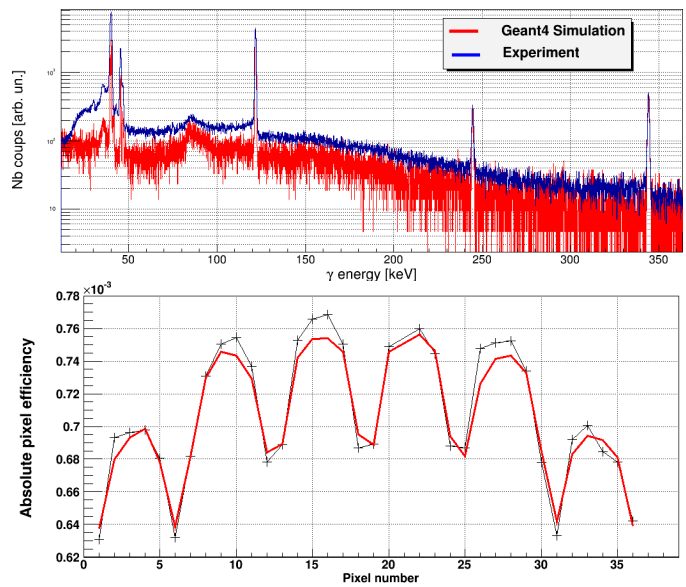


Figure 10. (Top) Gamma energy spectrum for a  $^{152}\text{Eu}$ , measured with the segmented ge detector (blue) compared to the Geant4 simulation (normalized to the number of counts at high energy). The difference in shape at low energy comes from electronic sources, not simulated by Geant4. (Bottom) Comparison of simulated (red line) and measured (black crosses) absolute efficiency of pixels at 122 keV.

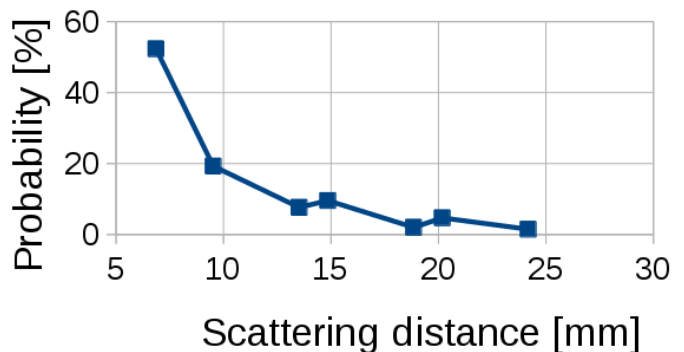


Figure 11. Distribution of scattering distance for one gamma event simulated in Geant4 for which a multiplicity of pixel larger than one got hit. 50 % of the events are scattered to the most neighboring pixel; but the scattering distance can be up to 3 or 4 pixels away.

controlled magnetic field to guide the electrons to a detector.

Geant4 simulations were done to assess the potential of such a system (Fig. 12) and showed that a 2 % absolute efficiency can be obtained for electrons, leading to an improvement factor around 10 to 20 times better than with  $\gamma$  rays detected with GRAPhEME. Following these simulations, a test setup will be built in collaboration with IFIN-HH and IRMM in the framework of the CHANDA project [22].



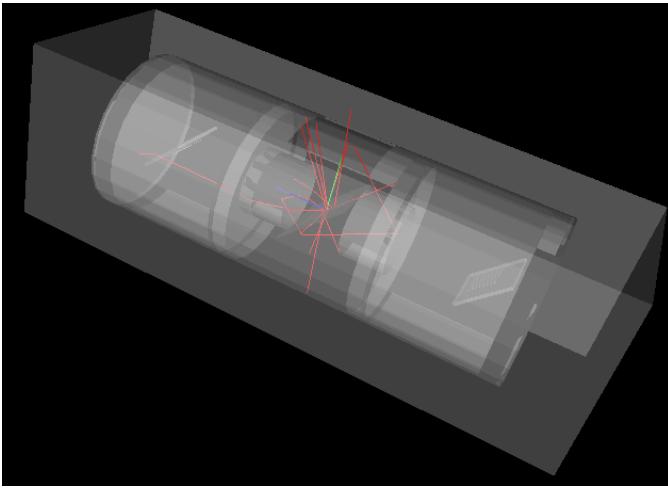


Figure 12. Simulated geometry of the conversion electron detection system in project. The red lines visualize the trajectory of some electrons emitted from the target.

### B. $^{233}\text{U}$ and very radioactive isotopes study

In the coming years, the recently upgraded GRAPhEME setup will be used to study  $^{233}\text{U}$  and  $^{239}\text{Pu}$ . A 8.3 g sample of  $^{233}\text{U}$ , in the form of a 30 mm diameter disk, 0.64 mm thick encased in a special made support, was placed in the setup between November 2014 and February 2015. After a total of about 700 hours of neutron beam, some (n, n') transitions already appear in the recorded gamma spectra. Following this study of  $^{233}\text{U}$ , developments are in progress in collaboration with the IRMM, and ITU to produce a  $^{239}\text{Pu}$  target that will be studied in the future.

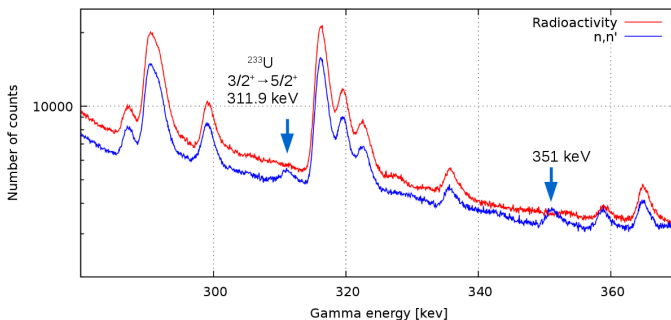


Figure 13. Preliminary spectra from  $^{233}\text{U}$  data study with GRAPhEME. The radioactivity window (red) does not show two peaks at 311.9 keV and 351 keV that appear in the (n, n') window.

## CONCLUSION

The GRAPhEME setup is dedicated to the study of (n, xn $\gamma$ ) reactions in actinides. It has been used to measure cross sections in isotopes of U, Th, W

and Zr. The comparison of experimental data to theoretical predictions provides insights on models weaknesses.

A recent upgrade, including the addition of a segmented germanium detector, has been made to the setup. This will allow the study of very radioactive isotopes like  $^{233}\text{U}$  and  $^{239}\text{Pu}$ .

In addition, for the study of strongly converted transitions, a system of conversion electron spectroscopy is currently understudy.

## ACKNOWLEDGMENTS

The authors thank the team of the GELINA facility for the preparation of the neutron beam, the IRMM target laboratory for their help in the samples preparation and the technical team at IRMM and IPHC for their support. This work was supported in part by the European Commission within the Seventh Framework Programme through CHANDA, under EURATOM contract no. FP7-605203.

## REFERENCES

- [1] M. Salvatores, R. Jacquemin, and al., "Uncertainty and target accuracy assessment for innovative systems using recent covariance data evaluations," OECD/NEA, Tech. Rep., 2008.
- [2] "IAEA nuclear data services website." [Online]. Available: <http://www-nds.iaea.org/exfor/>
- [3] D. Tronc, J. Salomé, and K. Böckhoff, "A new pulse compression system for intense relativistic electron beams," *Nuclear Instruments and Methods in Physics Research Section A: Accelerators, Spectrometers, Detectors and Associated Equipment*, vol. 228, no. 2–3, pp. 217 – 227, 1985. [Online]. Available: <http://www.sciencedirect.com/science/article/pii/0168900285902633>
- [4] D. Ene, C. Borcea, S. Kopecky, W. Mondelaers, A. Negret, and A. Plompen, "Global characterisation of the gelina facility for high-resolution neutron time-of-flight measurements by monte carlo simulations," *Nuclear Instruments and Methods in Physics Research Section A: Accelerators, Spectrometers, Detectors and Associated Equipment*, vol. 618, no. 1–3, pp. 54 – 68, 2010. [Online]. Available: <http://www.sciencedirect.com/science/article/pii/S0168900210005589>
- [5] J. Thiry, "Measurement of (n,xn $\gamma$ ) reaction cross sections of interest for the generation IV reactors," Ph.D. dissertation, Université de Strasbourg, 2010. [Online]. Available: <http://scd-theses.u-strasbg.fr/2016/>
- [6] M. Mosconi, R. Nolte, A. Plompen, C. Rouki, M. Kerveno, P. Dessagne, and J. Thiry, edited by E. Chiaveri (CERN, Geneva, Switzerland, 2010), September 2010.
- [7] "TNT digital pulse processor." [Online]. Available: <http://www.iphc.cnrs.fr/-TNT-.html>
- [8] L. Arnold, R. Baumann, E. Chambit, M. Filliger, C. Fuchs, C. Kieber, D. Klein, P. Medina, C. Parisel, M. Richer, C. Santos, and C. Weber, "Tnt digital pulse processor," in *Proceedings of the 14th IEEE-NPSS Conference on Real Time*, ser. RTC'05. Washington, DC, USA: IEEE Computer Society, 2005, pp. 265–269. [Online]. Available: <http://dl.acm.org/citation.cfm?id=1867821.1867881>

- [9] V. T. Jordanov and G. F. Knoll, “Digital synthesis of pulse shapes in real time for high resolution radiation spectroscopy,” *Nuclear Instruments and Methods in Physics Research Section A: Accelerators, Spectrometers, Detectors and Associated Equipment*, vol. 345, no. 2, pp. 337 – 345, 1994. [Online]. Available: <http://www.sciencedirect.com/science/article/pii/S0168900294910111>
- [10] C. Brune, “Gaussian quadrature applied to experimental  $\gamma$ -ray yields,” *Nuclear Instruments and Methods in Physics Research Section A: Accelerators, Spectrometers, Detectors and Associated Equipment*, vol. 493, no. 1–2, pp. 106 – 110, 2002. [Online]. Available: <http://www.sciencedirect.com/science/article/pii/S0168900202015528>
- [11] L. Mihailescu, L. Oláh, C. Borcea, and A. Plompen, “A new HPGe setup at Gelina for measurement of gamma-ray production cross-sections from inelastic neutron scattering,” *Nuclear Instruments and Methods in Physics Research Section A: Accelerators, Spectrometers, Detectors and Associated Equipment*, vol. 531, no. 3, pp. 375 – 391, 2004. [Online]. Available: <http://www.sciencedirect.com/science/article/pii/S0168900204011088>
- [12] “A General Monte Carlo N-Particle (MCNP) Transport Code.” [Online]. Available: <https://mcnp.lanl.gov/>
- [13] S. Agostinelli, J. Allison, K. Amako, and et al., “Geant4 — a simulation toolkit,” *Nuclear Instruments and Methods in Physics Research Section A: Accelerators, Spectrometers, Detectors and Associated Equipment*, vol. 506, no. 3, pp. 250 – 303, 2003. [Online]. Available: <http://www.sciencedirect.com/science/article/pii/S0168900203013688>
- [14] M. Kerveno, J. Thiry, A. Bacquias, C. Borcea, P. Dessagne, J. Drohé, S. Goriely, S. Hilaire, E. Jericha, H. Karam, A. Negret, A. Pavlik, A. Plompen, P. Romain, C. Rouki, G. Rudolf, and M. Stanoiu, “Measurement of  $^{235}\text{U}(n, n'\gamma)$  and  $^{235}\text{U}(n, 2n\gamma)$  reaction cross sections,” *Phys. Rev. C*, vol. 87, p. 024609, Feb 2013. [Online]. Available: <http://link.aps.org/doi/10.1103/PhysRevC.87.024609>
- [15] A. Bacquias, C. Borcea, P. Dessagne, M. Kerveno, J. C. Drohé, N. Nankov, A. L. Negret, M. Nyman, A. Plompen, C. Rouki, G. Rudolf, M. Stanoiu, and J. C. Thiry, “Study of  $(n, xn\gamma)$  reactions on  $^{235,238}\text{U}$ ,” 2012. [Online]. Available: <http://cds.cern.ch/record/1532351>
- [16] M. Kerveno, A. Bacquias, C. Borcea, P. Dessagne, J.-C. Drohé, N. Nankov, M. Nyman, A. Negret, A. Plompen, C. Rouki, G. Rudolf, M. Stanoiu, and J.-C. Thiry, “ $(n, xn\gamma)$  reaction cross section measurements for  $(n, xn)$  reaction studies,” *EPJ Web of Conferences*, vol. 42, p. 01005, 2013. [Online]. Available: <http://dx.doi.org/10.1051/epjconf/20134201005>
- [17] F. Belloni, “private communication.”
- [18] A. Koenig, S. Hilaire, and M. Duijvestijn, “TALYS a software package for the simulation of nuclear reactions.” [Online]. Available: <http://www.talys.eu/>
- [19] M. Herman, R. Capote, M. Sin, A. Trkov, B. Carlson, P. Obložinsky, C. Mattoon, H. Wienke, S. Hoblit, Y.-S. Cho, V. Plujko, and V. Zerkin, “Empire nuclear reaction model code.” [Online]. Available: <http://www.nndc.bnl.gov/empire>
- [20] G. Henning, “private communication.”
- [21] M. Dupuis, “private communication.”
- [22] “Solving Challenges in Nuclear Data.” [Online]. Available: <http://www.chanda-nd.eu/>